On measuring the contributions of various components to heat transfer in air

E.Yu. Shamparov[1*] and *I.N.* Zhagrina[1]

[1]The Kosygin State University of Russia, Moscow, Russia

Abstract. In the horizontal non-convective configuration, the thermal conductivity of an air volume bounded by polystyrene sidewalls and isothermal parallel surfaces of the heater and cooler was measured at thermal energy emissivities close to 0 or 1. In the vertical configuration, the maximum natural convection-induced increase in thermal conductivity of the same volume was measured, depending on the gap thickness between the heater and cooler. The relationships between radiative, conductive, and convective contributions to heat transfer were determined. The conditions for the onset of natural convection were investigated.

1 Introduction

Among the naturally occurring media around us, air is the most complex in terms of heat transfer properties. This complexity arises from the fact that air involves several distinct mechanisms that simultaneously play a significant role in heat transfer, and these mechanisms are interrelated. Consequently, heat transfer in air is referred to as "complex" [1].

Understanding the heat transfer properties of air is fundamental for developing insulation materials filled with it. In modern insulating materials, the volume occupied by air can reach 99% [2, 3]. Yet, in most cases, the developers of such materials are unfamiliar with the properties of air itself. Typically, the design of lightweight insulating materials is handled by specialists in "light industry materials science" or "construction materials science." However, their education lacks the fundamental depth required to work with "complex" heat transfer [4–6].

In this work, we demonstrate the diversity of air's heat transfer properties. We describe the apparatus and measurement techniques for characterizing these properties. We perform direct measurements of thermal resistance and optimize the structure, shape, and size of air-filled cells in the material. We present an alternative approach that can be effectively used in the development of "smart" ultralight insulating materials with a multiple-fold improvement in weight-per-unit-area to thermal resistance ratio.

Currently, the insulation market is overwhelmingly dominated by a "technological" approach. The foundation of this market for lightweight industrial and construction materials consists of foamed plastics or organic and mineral wools, produced in uniformly

* Corresponding author: shamparov-eu@rguk.ru

© The Authors, published by EDP Sciences. This is an open access article distributed under the terms of the Creative Commons Attribution License 4.0 (https://creativecommons.org/licenses/by/4.0/).

thick sheets. Structural engineering using these materials as semi-finished products has yet to emerge as a new development direction. Metallization [7] and other types of reflective coatings [8] are rarely used. An exception is foamed polyethylene, which is sometimes produced in combination with aluminum foil or metalized polyester film.

Among mass-produced lightweight insulating materials, expanded polystyrene (EPS) (density ~30 kg/m³, effective thermal conductivity [9] ~0.033 W/(m·K)) offers the best weight-per-unit-area to thermal resistance ratio. An additional advantage of EPS (foam) is its considerable mechanical strength. It is practically the only lightweight insulating material that can support its own weight and serve as a base for complex mechanical structures—a feature successfully utilized in packaging production. The technologies and equipment for shaping foam products into desired forms are readily available.

In this work, we demonstrate what the dimensions of air-filled cells in such an insulating structure should be—and why.

2 Problem statement

The ambient air atmosphere around us contains several heat transfer mechanisms simultaneously. We list them in order of their contribution magnitude:

Thermal radiation plays the dominant role in heat transfer within the atmosphere. Radiative heat transfer [10-12] is characterized by the medium's radiant thermal conductivity coefficient λ_r, which is directly proportional to its thermal radiation penetration depth a [1].

$$\lambda_r = 16\sigma T^3 a / 3, \tag{1}$$

where σ is the Stefan-Boltzmann constant and T is the absolute temperature of the medium. In air, the average thermal radiation penetration depth is approximately 3 kilometers [1].

In enclosed spaces, heat transfer via radiation is obstructed by walls. The radiation does not have sufficient place to interact with the air and instead transfers heat directly from hot walls to cold ones. Near an opaque wall, a temperature jump ΔT forms, equal to the difference between the wall temperature and the radiation temperature inside the enclosure, and proportional to the radiative heat flux density J_r:

$$J_r = Z_w \Delta T = \Delta T / R_w. \tag{2}$$

The wall is characterized by its thermal conductance Z_w (or its inversely proportional thermal resistance R_w), which amounts to [1]

$$Z_w = \frac{16}{3}\sigma T^3 \left\langle \frac{\varepsilon}{2-\varepsilon} \right\rangle, \tag{3}$$

where ε is the thermal emissivity of the wall. According to Kirchhoff's law, the thermal emissivity equals the absorptivity. For a wall whose emissivity depends on the radiation frequency ω,

$$\gamma = \left\langle \frac{\varepsilon}{2-\varepsilon} \right\rangle = \left(\int_0^\infty \frac{\varepsilon}{2-\varepsilon} f' \, \mathrm{d}\omega \right) / \left(4\sigma T^3 \right), \tag{4}$$

where f is the spectral power density of blackbody radiation (the Planck function).

$$\int_0^\infty f \, \mathrm{d}\omega = \sigma T^4, \; f' = \mathrm{d}f / \mathrm{d}T. \tag{5}$$

In simple cases: for a perfectly reflecting (mirrored) wall $\varepsilon \approx 0$ and $\gamma \approx 0$, for a black wall - $\varepsilon \approx 1$ and $\gamma \approx 1$, for a transparent and diffusely scattering partition - $\varepsilon \approx 1/2$ and $\gamma \approx 1/3$.

The second most significant heat transfer mechanism is forced convection (wind). Essentially, this is a manifestation of natural convection (see point 4) but not on the scale of enclosed volumes (rooms), rather on the scale of the entire atmosphere. Within the scope of the problem addressed in this work, this mechanism is irrelevant. Heat transfer to air passing through the space can be prevented using airtight partitions.

The third mechanism is heat transfer through evaporation and condensation of moisture. In our problem, it also plays no role.

The fourth mechanism is natural convection [13, 14], which arises by itself even in hermetically sealed volumes. Heat transfer occurs due to the movement of the medium (air). Near a hot wall, air heats up and absorbs heat, while near a cold wall it releases it. Hot air has lower density and therefore rises under the action of Archimedean force. Cold air, conversely, descends. Air movement is hindered by viscosity, which slows it down near stationary walls.

Natural convection is the most difficult heat transfer mechanism to describe. An analytical solution to the problem does not yet exist, even for the simple geometry we are using. And numerical solutions using ready-made programs work under the approximation when the thickness of the near-surface layer [13, 15, 16] is much smaller than the object's dimensions, meaning at high convection. We investigate and attempt to minimize the contribution of natural convection to heat transfer at maximum air cell sizes in the material. Therefore, direct experimental measurements are one of the most promising ways to obtain reliable information about the contribution ratios of different mechanisms to overall heat transfer in air.

According to Newton's law of viscosity, the flow velocity of the medium immediately adjacent to walls equals zero. Therefore, heat is transferred from walls to the medium only through conduction [13] (see point 5). In reality, natural convection never occurs by itself; instead, convective-conductive heat transfer is realized.

And only the fifth most significant heat transfer mechanism in air is conduction. It is proper to call conduction (not thermal conductivity) [1, 17-19] the heat transfer caused by diffusion of molecular kinetic energy transmitted through mutual collisions. For this heat transfer mechanism, Fourier's equation is valid. Here, the conductive heat flux density:

$$J_c = \mathrm{d}W_c / \mathrm{d}s \tag{6}$$

is proportional to the temperature gradient of the medium

$$J_c = -\lambda_c \nabla T, \tag{7}$$

where W_c is the conductive heat flux, s is the area it acts upon, and λ_c is the coefficient of conductive thermal conductivity of the medium.

In solid and liquid media, conduction is typically the dominant heat transfer mechanism. The coefficient of conductive thermal conductivity of air (equal to 0.025 W/(m·K) [1] under normal conditions) is orders of magnitude smaller than that of any solid or liquid substances. In lightweight insulating materials, radiative-conductive heat transfer is observed [17-19]. However, it is not conduction that determines the heat transfer properties of air.

For instance, in radiative heat transfer within a medium, the same form of law (7) holds true as in conductive transfer [1]. Moreover, the coefficient of radiant thermal conductivity of air λ_r is a million times greater [1] than the coefficient of conductive thermal conductivity λ_c.

The experiments were conducted using our specially developed "Apparatus for Non-Convective Measurements of Thermal Permeability of Materials" [20]. The configuration of the apparatus components in the "non-convective" mode is shown in Figure 1a.

A cooler (2) is horizontally positioned on the base platform (1). A foam cap (3) is placed over the platform, beneath which the heater (4) is fixed. Inside the cap, there is a thermal shield made of thick (0.5 mm) copper foil. The test sample is placed in the working zone of the apparatus between the heater and the cooler.

Both the cooler and heater have the same square shape with a side length of 85 mm (area $s_e = 7.23 \times 10^{-3}$ m²). The working surfaces of the cooler and heater consist of monocrystalline silicon plates (0.4 mm thick).

In the cooler, the silicon is bonded to a ceramic plate (aluminum oxide), which is, in turn, attached to a water-cooled copper radiator.

The heater is a double-sided copper-clad fiberglass board, with circuit traces on the lower side and uniformly distributed chip resistors soldered across the surface. The distributed heater has an electrical resistance $r_h = 20.0$ Ω.

The board is encapsulated in epoxy adhesive filled with quartz powder, ensuring no voids, and the silicon is securely bonded.

The design ensures:

Uniform temperature distribution across the entire heater (and cooler) surface.

A blackbody-like working surface (with emissivity $\varepsilon \approx 1$).

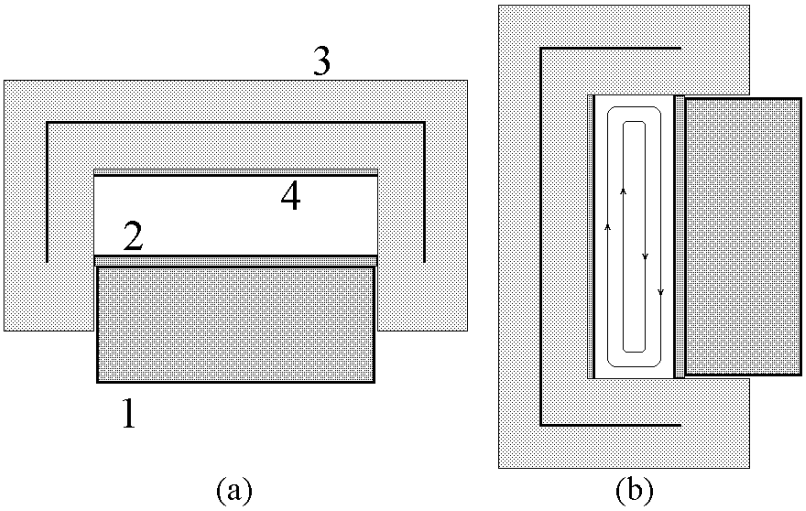

Fig. 1. Arrangement of components in the measurement setup

During measurements, we fix the gap thickness between the heater and cooler at a predetermined value. Using an electronic thermostat, we maintain the shield temperature at a set level (typically 50°C). We increase the power dissipated in the heater and, by adjusting the applied voltage, achieve a steady state where the heater temperature remains constant and equals the shield temperature. At this point, the heat flux from the heater to the shield becomes negligible due to two factors:

First, because of the expanded polystyrene thermal insulation between them.

Second, because their temperature difference approaches zero.

Therefore, nearly all power W_h generated in the heater,

$$W_h = U_h^2 / r_h, \tag{8}$$

flows through the sample to the cooler. By recording the steady-state values of the heater voltage U_h, and the temperatures of the heater T_h and cooler T_c, we can determine the thermal conductance of the sample Z_s,

$$Z_s = \frac{W_h}{s_e \left(T_h - T_c\right)}, \tag{9}$$

for a given sample thickness d.

3 Results and discussion

In the first series of measurements with horizontal configuration (Fig. 1a), air served as the sample. In general case, small enclosed air volumes exhibit parallel radiative and conductive-convective heat transfer mechanisms. However, in this particular configuration, the hot air is already positioned above the cold air and cannot rise further. Therefore, convection is explicitly absent.

For parallel radiative and conductive heat transfer, theoretical considerations (3, 7, 9) predict the thermal conductance should be:

$$Z_s = 8\sigma T_0^3 \gamma / 3 + \lambda_c / d, \tag{10}$$

where T_0 is the average of heater and cooler temperatures (314.9 K). Accordingly, Figure 2 presents the dependence of measured thermal conductance on inverse thickness $1/d$.

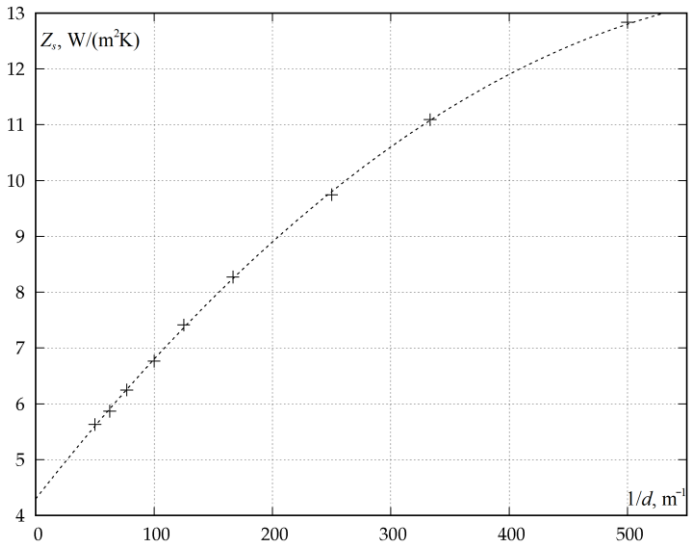

Fig. 2. Dependence of thermal conductance of the air gap on its inverse thickness

For large d, the data points fall as expected on the predicted straight line. However, at small thicknesses we observe a systematic measurement error. We believe this is related to the position of temperature sensors behind the silicon plates and at the periphery of the setup's working zone. Despite the uniform distribution of heat sources across the heater area, edge effects cause temperature differences between the center and periphery of the heater (cooler). This effect is proportional to the power dissipated in the heater and inversely proportional to the gap thickness.

Therefore, to eliminate the systematic error, we approximated the data with the best-fit dependence of the form:

$$Z_s = A + B/d - C/d^2$$

(shown as a parabola in the figure). The obtained parameters of the dependence are A = 4.3 W/(m^{2}K), B = 0.027 W/(m·K), and $C = 2\times10^{-5}$ W/K. Note that $8\sigma T_0^3/3$ = 4.72 W/(m^{2}K). Then $\gamma \approx 4.3/4.72 = 0.91$, and the emissivity of the heater and cooler surfaces (4) $\varepsilon = 2\gamma/(1+\gamma) \approx 0.95$, which agrees perfectly with our expectations. Additionally, the conductive thermal conductivity coefficient of air $\lambda_c \approx B$ = 0.027 W/(m·K) matches almost exactly the reference value at our measurement temperature [1].

In the second series of measurements, the working surfaces of the heater and cooler were covered with new thin (10 μm) aluminum foil using drops of sugar syrup. To avoid contaminating the surface, the foil was handled only with tweezers or through cotton fabric. The foil is made of very pure aluminum. The oxide layer on it is extremely thin. The emissivity of such surface is close to zero. The measurement results are presented in Figure 3.

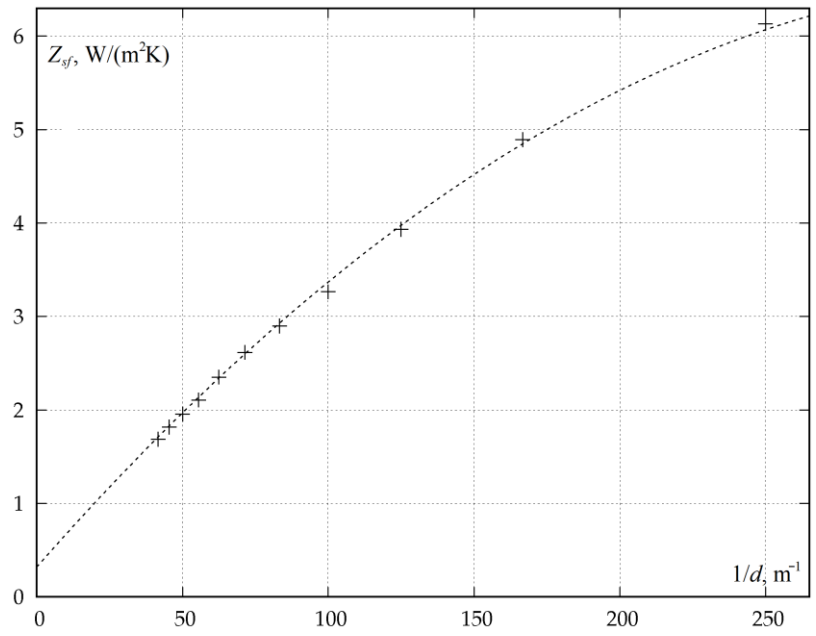

Fig. 3. Dependence of thermal conductance of the air gap on its inverse thickness when the heater and cooler are foil-covered

The figure also shows the approximating dependence $Z_{sf} \approx 0.32 + 0.0355/d - 0.00005/d^2$. By using the foil, we managed to reduce radiative heat transfer by approximately 14 times. The remaining noticeable radiative contribution of about 0.32

W/(m^{2}K) we attribute not to the foil's emissivity, but to radiation from the expanded polystyrene side walls.

In the third measurement series, we kept the foil but changed the measurement configuration from horizontal to vertical, as shown in Figure 1b. The results of thermal conductance Z_{sfc} measurements are presented in Figure 4a. For comparison, the approximating curve from the second measurement series is also shown there. Figure 4b shows the addition $Z_{sfc} - Z_{sf}$ contributed to thermal conductance by convection, plotted against gap thickness d.

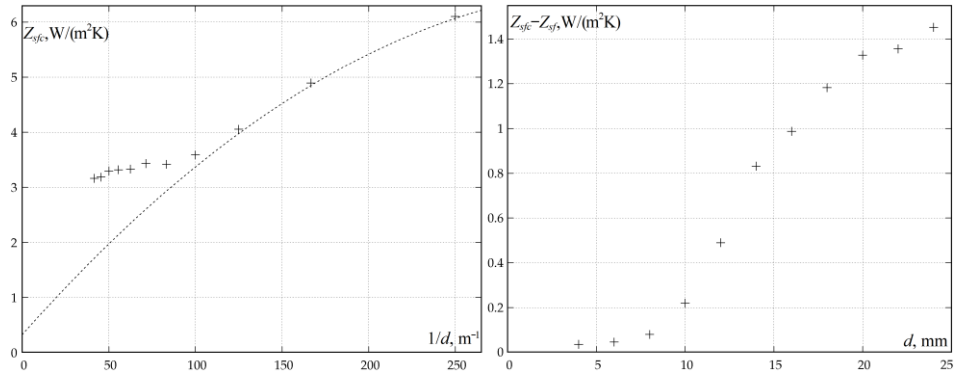

Fig. 4. Dependence of thermal conductance of the air gap on its inverse thickness when the heater and cooler are foil-covered in vertical configuration (a), and convective contribution to thermal conductance (b)

The vertical configuration provides maximum height where heated air rises near the heater and cold air sinks near the cooler. This is illustrated in Figure 1b. Among all possible rotation angles of the setup's working zone, this position should yield the maximum convective contribution.

It is evident that at small gap thicknesses, the convective contribution is negligible. Viscosity keeps the air stationary. For thicknesses between 10 and 18 mm, the contribution increases sharply as the air accelerates. Subsequently, the contribution shows a tendency to saturate. The accelerated near-surface air layer manages to absorb nearly all heat from the heater or deliver heat to the cooler, while a broad central region with nearly uniform temperature begins to form [15].

The maximum increase in convective contribution is observed at a gap thickness of 14 mm. Accordingly, 7 mm represents the effective thickness of the near-surface layer. The entire convective addition (approximately 2 W/(m^{2}K)) from the hot wall to the cold wall can be transported by air moving with an average velocity of about 20 cm/s. At such low velocities, the air flow can be considered laminar.

4 Conclusions

Thus, we have demonstrated the capability to measure radiative, conductive, and convective components of heat transfer in air. The relationships between the contributions of these components have been determined. For "black-walled" air cells, the radiative heat transfer component exceeds the conductive component at gap thicknesses as small as 5 mm. However, using highly reflective shields can reduce the radiative component by a factor of 10 or more. In this case, the radiative component becomes significant only at gap thicknesses exceeding 50 mm.

In vertical configurations with gap thicknesses below 10 mm, the convective component remains small. Beyond this thickness, it begins to increase rapidly. Notably, the thermal conductance of the air sample shows almost no decrease with increasing gap thickness, while its effective thermal conductivity increases proportionally with thickness.

It should be emphasized that, considering the role of boundary walls, our experimental setup effectively models the behavior of air cells in foam structures (insulation panels). The optimal gap thickness for constructing such ultralight insulating materials falls within the 10-13 mm range. This configuration maximizes the advantages of air - its low thermal conductivity and negligible weight - while keeping the contributions of radiation and convection relatively small.

At 10 mm thickness, our air sample with aluminum shields demonstrates an effective thermal conductivity of 0.035 W/(m·K), comparable to that of expanded polystyrene. However, a 1 cm layer of foam weighs five times more than two layers of our aluminum foil. Furthermore, the foil could be replaced with genuine metallized polyester film (3 μm thick), which weighs six times less still. For practically complete reflection, an aluminum layer of merely 100 nm thickness suffices [7]. Currently, such thin layers are deposited through vacuum coating processes, making these films substantially more expensive than conventional foil.

In conclusion, we have demonstrated the practical value of understanding complex heat transfer phenomena in air, which enables the design and optimization of smart air-filled materials with tailored composition and structure.

References

1. E. Shamparov, S. Rode, A. Bugrimov and I. Zhagrina, Analytical Solution of Problems about the Radiative and Radiative-Conductive Stationary Heat Transfer in a Medium with an Arbitrary Dependence of the Scattering and Absorption on Frequency. Boundary Conditions Energies **14,** 6339 (2021). https://doi.org/10.3390/en14196339
2. J.-J. Zhao, Y.-Y. Duan, X.-Dong Wang, Bu-Xuan Wang, Radiative properties and heat transfer characteristics of fiber-loaded silica aerogel composites for thermal insulation, International Journal of Heat and Mass Transfer **55,** 5196-5204 (2012). http://dx.doi.org/10.1016/j.ijheatmasstransfer.2012.05.022
3. Y. Liang, Y. Wang, H. Wu, G. Huang, J. Yang, Controllable nano-fibrous interlayers for improved thermal insulation performance, Applied Thermal Engineering **179,** 115781 (2020). https://doi.org/10.1016/j.applthermaleng.2020.115781
4. A. Lakatos, A. Csík, E. Lucchi, A. D. La Rosa, Thermal performance and ageing effects to model the life cycle assessment of heat-protective thermal insulation materials in pipe systems, International Communications in Heat and Mass Transfer **164**, 108819 (2025). https://doi.org/10.1016/j.icheatmasstransfer.2025.108819
5. C. Gaunand, Y. De Wilde, A. François, V. Grigorova-Moutiers, K. Joulain, Modeling conductive thermal transport in three-dimensional fibrous media with fiber-to-fiber contacts, Physical Review Applied **23**, 3, 034084 (2025). https://doi.org/10.1103/PhysRevApplied.23.034084
6. A. Angelotti, A. Alongi, A. Augello,A. Dama, S. De Antonellis, A. Ravidà, M. Zinzi, E. De Angelis, Thermal conductivity assessment of cotton fibers from apparel recycling for building insulation, Energy and Buildings **324**, 114866 (2024). https://doi.org/10.1016/j.enbuild.2024.114866
7. N. Yüksel, A. Avcı, M. Kılıç, The temperature dependence of effective thermal conductivity of the samples of glass wool reinforced with aluminium foil, International

Communications in Heat and Mass Transfer **37,** 675-680 (2010). https://doi.org/10.1016/j.icheatmasstransfer.2010.02.004

8. W. Yuan, Y. Song, H. Liu, P. Han, P. Chu, Y. Liu, W. Xie, K. Yu, W. Zu, C. Bian, Z. Peng, Multifunctional coral-like thermal radiation shielding MoSi2/SiC fibers: Favourable thermal insulation, oxidation resistant and mechanical properties, Ceramics International **069** (2025). https://doi.org/10.1016/j.ceramint.2025.02.069
9. M.K. Choudhary, W. Eastes, Effective thermal conductivity of fiberglass insulation, International Journal of Applied Glass Science **15,** 3, 307-316 (2024). https://doi.org/10.1111/ijag.16652
10. A. Tilioua, L. Libessart, G. Jeandel, S. Lassue, Determination of radiative properties of polyester batting insulation material from hemispherical transmittance and reflectance measurements, Applied Thermal Engineering **105,** 594-604 (2016). https://doi.org/10.1016/j.applthermaleng.2016.03.050
11. A. Celzard, G. Tondi, D. Lacroix, G. Jeandel, B. Monod, V. Fierro, A. Pizzi, Radiative properties of tannin-based, glasslike, carbon foams, CARBON **50**, 4102-4113 (2012). https://doi.org/10.1016/j.carbon.2012.03.029
12. J. Sorel Djeumegni, M. Lazard, V. Le Dez, H. Thierry T. Kamdem, Radiative heat transfer in a 2D semi-transparent gray medium with a centered inner square cavity, International Journal of Heat and Mass Transfer **149,** 119209 (2020). https://doi.org/10.1016/j.ijheatmasstransfer.2019.119209
13. F. Lafta Rashid, H.I. Mohammed, A. Dulaimi, M.A. Al-Obaidi, P. Talebizadehsardari, Shabbir Ahmad, Arman Ameen, Analysis of heat transfer in various cavity geometries with and without nano-enhanced phase change material: A review, Energy Reports **10,** 3757-3779 (2023). https://doi.org/10.1016/j.egyr.2023.10.036
14. E. Momoniat, C. Harley, R.S. Herbst, Effects of extended surfaces on heat transfer in buoyancy-driven flow in a square cavity, Results in Engineering **18,** 101190 (2023). https://doi.org/10.1016/j.rineng.2023.101190
15. N. Ouertatani, N. Ben Cheikh, B. Ben Beya, T. Lili, Numerical simulation of two-dimensional Rayleigh–Bénard convection in an enclosure, Comptes Rendus Mécanique **336,** 5, 464-470 (2008). https://doi.org/10.1016/j.crme.2008.02.004
16. Pranowo, Agung Tri Wijayanta, Numerical solution strategy for natural convection problems in a triangular cavity using a direct meshless local Petrov-Galerkin method combined with an implicit artificial-compressibility model, Engineering Analysis with Boundary Elements **126**, 13-29 (2021). https://doi.org/10.1016/j.enganabound.2021.02.006
17. R. Arambakam, H. Vahedi Tafreshi, B. Pourdeyhimi, Modeling performance of multi-component fibrous insulations against conductive and radiative heat transfer, International Journal of Heat and Mass Transfer **71**, 341-348 (2014). http://dx.doi.org/10.1016/j.ijheatmasstransfer.2013.12.031
18. S.-Y. Zhao, B.-M. Zhang, S.-Y. Du, An inverse analysis to determine conductive and radiative properties of a fibrous medium, Journal of Quantitative Spectroscopy & Radiative Transfer **110**, 1111-1123 (2009). https://doi.org/10.1016/j.jqsrt.2009.03.022
19. A. Kaemmerlen, F. Asllanaj, H. Sallée, D. Baillis, G. Jeandel, Transient modeling of combined conduction and radiation in wood fibre insulation and comparison with experimental data, International Journal of Thermal Sciences, **49** (11), 2169-2176 (2010). https://doi.org/10.1016/j.ijthermalsci.2010.06.013
20. E.Yu. Shamparov, I.N. Zhagrina, RF Utility Model No.166709 (2016)